International Journal of Antimicrobial Agents 64 (2024) 107200

Contents lists available at ScienceDirect

International Journal of Antimicrobial Agents

journal homepage: www.elsevier.com/locate/ijantimicag

Plasma, Intracellular and Lymph Node Antiretroviral Concentrations and HIV DNA Change During Primary HIV Infection: Results from the INACTION P25 Study

Amedeo De Nicolò[1,#,*], Alice Palermiti[1,#], Stefania Dispinseri[2], Giulia Marchetti[3], Mattia Trunfio[4], Elisa De Vivo[1], Antonio D'Avolio[1], Antonio Muscatello[5], Andrea Gori[5], Stefano Rusconi[6,7], Elena Bruzzesi[8], Arianna Gabrieli[9], Davide Paolo Bernasconi[10], Alessandra Bandera[7], Silvia Nozza[11], Andrea Calcagno[4], on behalf of the INACTION (Italian Network of Acute HIV Infection) study group

[1] *Laboratory of Clinical Pharmacology and Pharmacogenetics, Department of Medical Sciences, University of Turin, Turin*
[2] *Viral Evolution and Transmission Unit, IRCCS Ospedale San Raffaele, Milan*
[3] *Clinic of Infectious Diseases, Department of Health Sciences, ASST Santi Paolo e Carlo, University of Milan, Milan*
[4] *Unit of Infectious Diseases, Department of Medical Sciences, University of Turin, Turin*
[5] *Infectious Diseases Unit, Foundation IRCCS Ca' Granda Ospedale Maggiore Policlinico, Milan*
[6] *UOC Malattie Infettive, Ospedale Civile di Legnano, ASST Ovest Milanese, Legnano*
[7] *University of Milan, Milan*
[8] *Vita-Saluta San Raffaele University, Milan*
[9] *Dipartimento di Scienze Biomediche e Cliniche, Ospedale L Sacco, Milan*
[10] *Bicocca Bioinformatics Biostatistics and Bioimaging Centre - B4 School of Medicine and Surgery, University of Milano-Bicocca, Monza*
[11] *Department of Infectious Diseases, IRCCS Ospedale san Raffaele, Milan, Italy*

ARTICLE INFO

Article history:
Received 13 October 2023
Accepted 7 May 2024

Editor: D. Cluck

Keywords:
Acute HIV infection
Primary HIV infection
Antiretroviral therapy
Intracellular
Tissue
Pharmacokinetics

ABSTRACT

Despite its effectiveness, combination antiretroviral treatment (cART) has a limited effect on HIV DNA reservoir, which establishes early during primary HIV infection (PHI) and is maintained by latency, homeostatic T-cells proliferation, and residual replication. This limited effect can be associated with low drug exposure in lymphoid tissues and/or suboptimal adherence to antiretroviral drugs (ARVs). The aim of this study was to assess ARV concentrations in plasma, peripheral blood mononuclear cells (PBMCs) and lymph nodes (LNs), and their association to HIV RNA and HIV DNA decay during PHI. Participants were randomised to receive standard doses of darunavir/cobicistat (Arm I), dolutegravir (Arm II) or both (Arm III), with a backbone of tenofovir alafenamide and emtricitabine. Total HIV DNA was measured using digital-droplet PCR in PBMCs at baseline, 12 and 48 weeks. Drug concentrations in plasma and PBMCs were determined at 2, 12 and 48 weeks (LNs at 12 weeks) by UHPLC-MS/MS. Seventy-two participants were enrolled, mostly male (n=68), with a median age of 34 years and variable Fiebig stages (V–VI 57.7%, I–II 23.9%, and III–IV 18.3%). Twenty-six patients were assigned to Arm I, 27 to Arm II and 19 to Arm III. After 48 weeks, most patients had undetectable viremia, with minor differences in HIV RNA decay between arms. Patients with Fiebig I–II showed faster HIV RNA and HIV DNA decay. Intracellular tissue penetration was high for nucleoside analogues and low-moderate for darunavir and dolutegravir. Only tenofovir diphosphate concentrations in PBMCs showed correlation with HIV DNA decay. Overall, these results indicate that the timing of treatment initiation and intracellular tenofovir penetration are primary and secondary factors, respectively, affecting HIV reservoir.

* Corresponding author: Amedeo De Nicolò, Laboratory of Clinical Pharmacology and Pharmacogenetics*. University of Turin, Department of Medical Sciences, Amedeo di Savoia Hospital, Corso Svizzera 164 - 10149 - TURIN (ITALY) *UNI EN ISO 9001 and 13485 Certified Laboratory; Web Site: www.tdm-torino.org.
E-mail address: amedeo.denicolo@unito.it (A. De Nicolò).
# These authors contributed equally to this paper.

https://doi.org/10.1016/j.ijantimicag.2024.107200

1. Introduction

The persistence of HIV in cells and in protected organs and tissues is one of the key reasons why HIV can be pharmacologically controlled but not eradicated in people living with HIV (PLWH) [1–4]. Several factors sustain HIV persistence during combination antiretroviral treatment (cART), including proviral HIV DNA latency, homeostatic proliferation of infected T-cells and residual replication [3,5–9], leading to an extremely slow and limited decay of the HIV DNA reservoir during treatment [1,10,11]. Different curative strategies are currently being tested, including the reactivation of latently infected cells along with immune system enhancing treatments, known as the "kick and kill" strategy [12,13]; the epigenetic inhibition of viral transcription, known as the "block and lock" approach [14–16], and "gene editing" therapies that modify proviral DNA to make it replication-incompetent [8,17–20]. Despite significant research efforts, so far only allogenic bone marrow transplant from donors with homozygous CCR5 gene deletion (in 3 individuals to date) [21–24], and treatment during acute infection have been associated with virological control after treatment interruption [25–28]. Primary HIV infection (PHI) is a rarely diagnosed condition where early treatment has been associated with improved clinical, immunological, and virological outcomes and, in approximately 8% (5–15%) of patients in a French cohort, post-treatment control (i.e., virological control without ARVs after a period of cART) [27,28]. Albeit promising, these results only highlighted a subset of patients that received antiretroviral treatment (ART) during PHI: randomised and controlled studies did not identify the most beneficial therapeutic regimen for patients diagnosed early after being infected with HIV [29].

Several tissues and organs have been listed as potential sites of continuous, and potentially differential, replication during suppressing ART (including central nervous system, lymph nodes [LNs], spleen, and gut/gut-associated lymphoid tissue) [2,4,6,8,30–32]. Recent studies have identified lymphoid tissues as sanctuary sites where ART penetration is limited and variable, and where HIV replication may persist [2,8,31,33]. Physicochemical characteristics associated with greater lymphatic system penetration were shown to be high molecular weight, larger particle size, log P value $>$ 5, and high long-chain triglycerides solubility [19,31]. Additional features potentially affecting drug passage in LNs are tissue fibrosis (observed in several PLWH), inflammation, and transporter expression and activity [34–36]. Published studies using different methods (hollow fibres, models, tissue homogenate, mononuclear cell extraction) suggested differential exposures in LNs as well as highly variable inhibitory quotients [30,31,37,38]. A trend towards lower LN HIV RNA was observed in the follow-up of patients treated during PHI with two nucleos(t)ide reverse transcriptase inhibitors (NRTIs) plus dolutegravir (DTG) and maraviroc, with the latter CCR5 inhibitor showing a peculiarly high LN penetration [30]. The aims of this sub-study were to quantify ARV concentrations in plasma, peripheral blood mononuclear cells (PBMCs) and LNs and to evaluate their association with HIV DNA decay up to week 48 after the introduction of ART in people treated during PHI with currently used common, potent combinations.

2. Material and methods

2.1. Enrolment, inclusion criteria and randomisation

Treatment-naïve adult participants diagnosed with PHI who gave written informed consent were included in this prospective, randomised, open-label, multicentre clinical study. The study received ethical approval from the Institutional Ethics Committee of the San Raffaele Hospital (coordinating centre).

Inclusion and exclusion criteria were described in detail in a previous work [39]. In particular, the self-reported adherence to treatment had to be higher than 95% throughout the study period. Moreover, an additional exclusion criterion was the observation of detectable tenofovir alafenamide (TAF) concentrations in plasma throughout the protocol. TAF should be undetectable at the end of the dosing interval (24 h, C_{trough}) as it is known to be rapidly converted during the first 8 h after the dose intake [40]. The detection of TAF in plasma can be a marker of suboptimal adherence to the timings of drug intake in the study protocol.

Patients were randomised in a ratio of 10:10:8 to receive one of the following three treatment regimens, all of which share a TAF and emtricitabine (FTC) nucleosidic backbone: darunavir boosted with cobicistat (DRV + COBI 800/150 mg QD; DRV/c) plus TAF/FTC 10/200 mg QD; dolutegravir (DTG, 50 mg QD) plus TAF/FTC 25/200 mg QD; or DTG + DRV/c + TAF/FTC (800/150 mg QD + 50 mg QD + 10/200 mg QD, respectively). These combinations were investigated because DTG is first-line, with good distribution, a high barrier to resistance and expected fast virological decline; and DRV has good CSF penetration, a high barrier to resistance and a post-transcriptional effect.

2.2. Clinical and Virological Follow-up

Virological and immunological parameters were monitored throughout the protocol. Plasma HIV RNA viral load (lower limit of quantification [LLOQ]: 25 copies/mL; limit of detection [LOD]: 20 copies/mL), as well as CD4+ lymphocytes count, were measured at baseline and at 2, 4, 8, 12, 24, 36, and 48 weeks of therapy. HIV RNA viral loads lower than the LLOQ were approximated to the LOD value of 20 copies/mL. HIV total proviral DNA (hereafter, HIV DNA) was quantified in PBMCs purified by density gradient, using a validated digital droplet PCR method (LLOQ 2 copies/million cells) at baseline, and 12 and 48 weeks.

2.3. Drug quantification in plasma, PBMCs and lymph nodes

All enrolled patients underwent blood sampling for the quantification of drug concentrations in plasma at the end of the dosing interval (C_{trough}) at 2, 4, 8, 12, 24, 36 and 48 weeks. Intra-PBMC concentrations were determined at 2, 12 and 48 weeks of treatment. PBMC isolates were obtained by density gradient with CPT tubes, which reduce the contamination by red blood cells, with a protocol with two fast washing steps with 0.9% NaCl at 4°C, as previously described [41,42].

Analytes were measured using validated UHPLC-MS/MS methods [42–44], based on the protein precipitation and the use of stable isotope-labelled internal standards (SIL-IS) for each analyte. LLOQ values for each drug in plasma and PBMCs were, respectively: 31 ng/mL and 0.39 ng/sample for DTG, 39 ng/mL and 0.039 ng/sample for DRV, and 10 ng/mL and 0.039 ng/sample for COBI. On the other hand, the quantification of TFV-diphosphate (TFV-DP) and FTC-triphosphate (FTC-TP) in PBMCs and LNs was performed using a validated HPLC-MS/MS method based on ion-coupling chromatography on a graphitic carbon column (Hypercarb ® 3 µm, 2.1 × 100 mm column) with a gradient of two mobile phases: water + 0.2% hexylamine and 5 mM of diethylamine + 2% of acetic acid (Mobile Phase A); and 60:40 vol:vol acetonitrile/mobile phase A (Mobile Phase B). The gradient run duration was 15 min at 40°C and the flow rate was 0.4 mL/min.

The method was validated following FDA and EMA guidelines on PBMC samples, showing satisfactory accuracy (trueness, bias $<$ 15%) and intra- and inter-day precision (coefficients of variation $<$ 15%), and reproducible matrix effect and recovery. The LLOQ for TFV–DP and FTC–TP was 0.039 ng/sample.

Intracellular drug amounts were then normalised by volume of cells in each sample, calculated by multiplying the cell numbers and a mean cell volume of 283 fL, as described previously [41], giving intracellular concentrations in ng/mL. Correcting the LLOQ values for the intracellular assays by a mean cell number per sample of 10 million (volume of 2.8 µL/sample), the intracellular LLOQ for all the drugs was 13.8 ng/mL.

The quantification in needle biopsies (approximately 10 mg of tissue) from inguinal LNs was performed in only a small subset of patients who agreed to undergo needle biopsies for viro-immunological and pharmacological purposes at 12 weeks of treatment, at the end of the dosing interval. In these samples, the quantification was performed after homogenisation, protein precipitation and UHPLC-MS/MS analysis. The observed drug amounts were corrected by sample weights, to give concentrations in ng/g.

To compare ratios of LNs to plasma and LNs to PBMCs, an approximate density for LNs of 1 g/mL was assumed, in accordance with a previous work and confirmed experimentally in our samples [45]. For the determination of ratios of intracellular TFV–DP and FTC–TP to plasma TFV and FTC concentrations, all the results were corrected by the molar ratios (TFV–DP/TFV and FTC–TP/FTC) of 0.642 and 0.507, respectively.

2.4. Statistical Analysis

The distribution of continuous variables was summarised using median and first–third quartile (interquartile range [IQR]), and categorical variables were reported as absolute number and percentage. Patient characteristics and virological parameters were compared between treatment arms using Kruskal-Wallis or Chi-square tests for continuous and categorical variables, respectively.

Friedman test was adopted to test the difference of the drug concentrations between time visits (weeks 2, 12 and 48). Spearman correlation index was used to evaluate the association between drug concentrations and HIV DNA change in time (at weeks 12 and 48).

Finally, the association between Fiebig stage (I–II vs. III–IV vs. V–VI) and the change in time of log-transformed HIV RNA (baseline, week 4, 8, 12, 24, 36, and 48) and log-transformed HIV DNA (baseline, week 12 and 48) was assessed using mixed-effects linear regression with participant as random effect.

3. Results

3.1. Patient baseline characteristics

A total of 78 patients were screened and 72 patients met the inclusion criteria. The six patients who did not meet the inclusion criteria showed detectable TAF concentrations in plasma, thus they were excluded from the analysis due to suspected suboptimal adherence to the timing of drug intake according to the protocol. Patient characteristics at baseline are reported in Table 1.

Most patients were male (68, 94.4%) and relatively young, with a median age of 34.1 years (IQR 28.3–43.9). Median baseline CD4+ cell count was 658 cells/mL (IQR 474–796); median HIV RNA in plasma was 5.66 $\log_{10}$ cps/mL (IQR 4.62–6.50) and HIV DNA in PBMCs was 4.46 $\log_{10}$ cps/10^6 PBMCs (IQR 4.08–4.81).

Patients were mostly diagnosed during Fiebig stages V–VI (57.7%), I–II (23.9%) and III–IV (18.3%).

3.2. Differences Between Arms

After randomisation, 26 patients were assigned to the DRV/c arm (Arm I), 27 to the DTG arm (Arm II) and 19 to the DTG + DRV/c arm (Arm III). There were no significant differences between study arms in baseline characteristics, CD4+ T-cell count reconstitution up to 48 weeks or HIV DNA change over time. Arm I (DRV) showed a slightly slower decay in plasma HIV RNA during the first 12 weeks compared with the other treatment arms. There were no significant differences between study arms in drug concentrations (for TFV and FTC) in plasma, PBMCs or LNs. Detailed data about differences between regimens have been published elsewhere [39].

Table 1
Participant characteristics at baseline.

Total no. of participants (n = 72)	
Randomisation Arms	
Arm I: DRV/c + TAF + FTC	I = 26
Arm II: DTG + TAF + FTC	II = 27
Arm III: DTG + DRV/c + TAF + FTC	III = 19
Sex (male/female)	68/4 (94.4%/5.6%)
Age, years (median, IQR)	34.1 (28.3–43.9)
Sexuality (n; %)	Heterosexual/Bisexual = 21 (29.2)
	MSM = 42 (58.3)
	Not reported = 9 (12.5)
Fiebig Stage (n; %)	I = 4 (5.5)
	II = 13 (18.1)
	III = 5 (6.9)
	IV = 9 (12.5)
	V = 29 (40.3)
	VI = 12 (16.7)
CD4+ count (cells/mm^3)	658 (IQR 474–796)
Plasma HIV-RNA (Log_{10} cps/mL)	5.66 (IQR 4.62–6.50)
Plasma HIV-DNA (Log_{10} cps/mL)	4.46 (IQR 4.08–4.81)

3.3. Drug concentrations in the compartments and correlation with virological effectiveness

Median trough concentrations in plasma, PBMCs and LNs (in a small subset of patients, n=9) for each ARV are summarised in Table 2 (PBMC- and tissue-to-plasma ratios are described in supplementary material). DTG plasma concentrations tended to increase over time, showing slightly higher concentrations at weeks 12 and 48 ($P = 0.097$), but there was no such trend in PBMCs ($P = 0.646$). All samples except for TAF showed quantifiable drug concentrations.

DTG and DRV penetration in PBMCs appeared limited, showing median ratios of 0.31 and 0.32, respectively, at 12 weeks of treatment. Conversely, TFV–DP and FTC–TP showed higher penetration in PBMCs (median ratios of 28.29 and 16.98, respectively) and whole-LNs (median ratios of 11.13 and 16.04, respectively).

Drug concentrations in plasma and PBMCs were mutually correlated for DTG, DRV and COBI (Spearman rho values between 0.366 and 0.789, *P*-values between 0.073 and < 0.001). Conversely, concentrations of TFV–DP and FTC–TP in PBMCs were not correlated to those in plasma (*P*-values > 0.075) at any timepoint.

3.4. PK/PD correlations

Testing the correlation between drug concentrations in plasma, PBMCs and LNs with HIV RNA and HIV DNA viral load change over time showed only borderline correlations of HIV DNA change at 48 weeks with TFV–DP concentration in PBMCs (r = -0.32; $P = 0.057$), and TFV–DP accumulation ratio in PBMC/plasma (r = -0.33; $P = 0.053$). This indicates that higher intracellular accumulation of TFV–DP was associated with higher decay in HIV DNA.

3.5. Effect of Fiebig stages on immunological/virological endpoints

As reported in Table 1, participants had variable Fiebig stage: the most common stages were II (13 patients, 18.3%), V (29 patients, 40.8%) and VI (12 patients, 16.9%). There were no significant differences between Fiebig stages in terms of baseline CD4+

Table 2
Summary of the observed drug concentrations in plasma, PBMC and LN homogenates throughout the protocol.

Drug	Week 2			Week 12				Week 48		
	Plasma (ng/mL)	PBMC (ng/mL)	PBMC (fmol/10^6 cells)	Plasma (ng/mL)	PBMC (ng/mL)	PBMC (fmol/10^6 cells)	LN* (ng/g)	Plasma (ng/mL)	PBMC (ng/mL)	PBMC (fmol/10^6 cells)
Median DTG conc. (IQR)	1213 (465–1911)	478 (114–1422)	323 (77–960)	1613 (1285–2306)	592 (301–1402)	400 (203–946)	851 (482–530)	1817 (1278–2344)	630 (381–1090)	425 (257–736)
Median DRV conc. (IQR)	2144 (1053–3191)	984 (403–4125)	509 (208–2132)	1887 (821–3192)	783 (285–1327)	405 (147–686)	983 (253–1890)	2120 (709–3700)	983 (281–2216)	508 (145–1146)
Median COBI conc. (IQR)	97 (35–382)	379 (111–1797)	138 (41–656)	126 (43–267)	299 (85–513)	109 (31–187)	49 (11–113)	188 (32–316)	798 (90–1199)	291 (32–438)
Median TFV conc. (IQR)	8.5 (7.2–11.5)	500 (202–778)	318 (128–494)	7.9 (6.5–10.6)	379 (190–576)	241 (121–366)	170 (49–452)	9.4 (7.8–12.8)	316 (100–556)	201 (64–353)
Median FTC conc. (IQR)	126 (56–195)	4074 (2432–6822)	2367 (1412–3964)	109 (68–202)	4330 (2120–6152)	2516 (1232–3574)	2532 (253–3667)	125 (75–285)	4342 (2282–7443)	2522 (1326–4324)

* LN concentration was determined on the whole-tissue homogenate, including intracellular and interstitial fluid concentrations. No normalisation by cell numbers can be performed.

cells count and recovery over time ($P > 0.641$). On the other hand, participants with lower Fiebig stages (I–II) had significantly higher plasma HIV RNA at baseline ($P = 0.001$) compared with participants diagnosed at later stages (III–VI). This difference was lost at follow-up, resulting in a significantly higher decay of plasma HIV RNA in participants diagnosed at Fiebig stages I–II (Figure 1, $P = 0.031$ vs. III–IV and $P < 0.001$ vs. V–VI).

Conversely, there were no differences in terms of HIV DNA in PBMC samples between Fiebig stages at baseline ($P = 0.739$), but this difference became increasingly important during treatment, reaching borderline significance at 48 weeks of treatment ($P = 0.068$). This significant trend was confirmed by mixed-modelling, which showed a significantly faster HIV DNA decay during treatment in patients with Fiebig stages I–II compared with stages III–IV ($P = 0.017$) and V–VI ($P = 0.005$), respectively. These results are depicted in Figure 2.

3.6. Interplay between Fiebig stages and cART

Once the impact of treatment arms and Fiebig stages on virological endpoints was observed, the aim was to understand the effect of cART, in terms of type of treatment and pharmacokinetic (PK) features, stratifying the participants in low (I–II) and high (III–VI) Fiebig stages. Patient characteristics during treatment are summarised divided by treatment arm in low (Table 3) and high (Table 4) Fiebig stages.

As shown, there are no significant differences in terms of CD4+ cell recovery, HIV RNA and HIV DNA kinetics between treatment arms in low Fiebig stages, whereas a significantly slower decay in HIV RNA viral load was observed in patients from Arm I (DRV) compared with the other arms (DTG and DRV+DTG) in patients with higher Fiebig stages (III–VI). In line with the previous associations between HIV DNA decay and PK/PD parameters, only TFV–DP concentration in PBMCs (r = -0.46; $P = 0.019$) and the TFV–DP PBMCs-to-plasma concentration ratio (r = -0.47; $P = 0.017$) were correlated with HIV DNA decay at week 48 in the higher Fiebig stages group. This correlation is depicted in Figure 3.

4. Discussion

The present randomised controlled study is one of the first to evaluate modern therapeutic choices for the treatment of PHI and to confirm the lack of effect of intensified regimens. The results from this study confirm the evidence from previous cohorts regarding the higher HIV DNA decay in PHI, particularly during the very early phases, namely Fiebig stages I–II [25].

There was a significantly faster decay in HIV RNA in the arms containing DTG (Arms II and III), but no difference in HIV DNA decay. This was more evident in the context of more advanced Fiebig stages (III–VI), but was not statistically significant in extremely early stages (Fiebig I–II).

The drugs that showed the highest penetration in PBMCs and LNs were the phosphorylated metabolites of the nucleoside analogues, TFV–DP, and FTC–TP, confirming previous reports and the well-known capability of TAF to accumulate in PBMCs [19,37,46]. On the other hand, both the “third drugs” (either DTG or DRV) showed PBMCs-to-plasma and LNs-to-plasma ratios lower than 1, highlighting a moderate penetration of these drugs in PBMCs and LNs. These results are higher (0.32 and 0.59, respectively) than those reported by Fletcher et al. in LN mononuclear cells (LNMCs) [19], where the reported DTG LNMC-to-plasma ratio was nearly 0.01. This difference was expected, as these studies aimed to describe drug concentrations in two different compartments. In the current work, tissue homogenates were used from inguinal LNs to describe the drug concentrations in the whole LN microenvironment, including interstitial fluid and different cell types. Therefore,

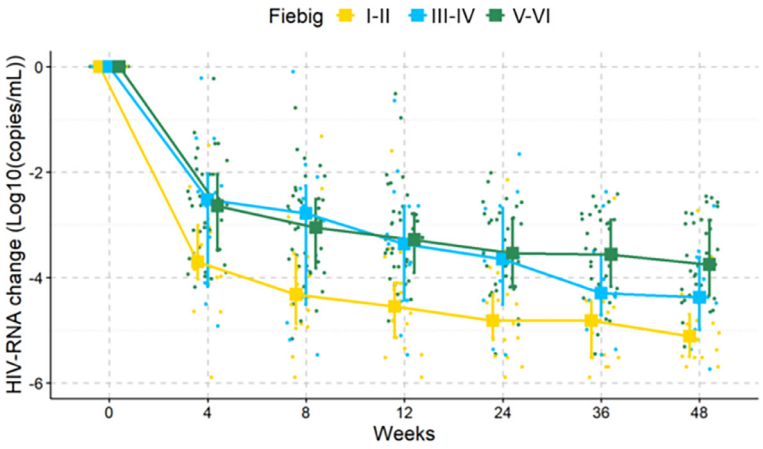

Figure 1. HIV RNA changes throughout the treatment period of 48 weeks, stratified by Fiebig stages.

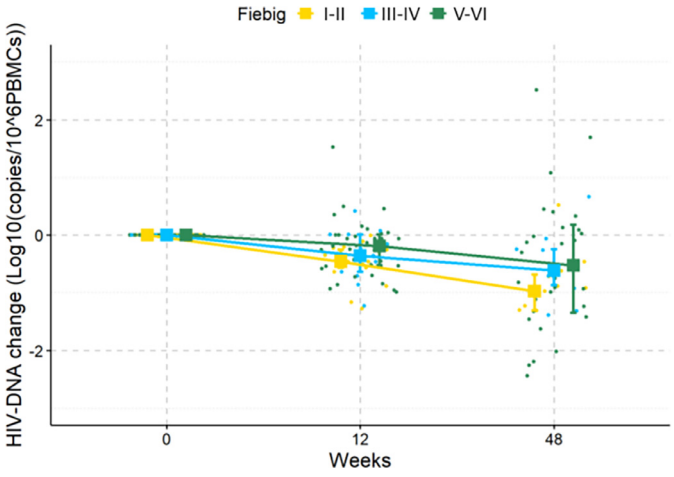

Figure 2. HIV DNA changes in peripheral blood mononuclear cells (PBMCs) during the study period, stratified by Fiebig stages.

these results cannot be directly compared to the intra-LNMC concentrations, particularly for drugs with limited intracellular penetration, such as DTG. This important difference between concentrations in LN homogenates (generally lower than concentrations in plasma for the "third drugs"), representing the microenvironment, and the literature-reported LNMC concentrations confirm lower than proportional penetration of DTG from the extracellular matrix in LNMCs compared with PBMCs (from blood/plasma). On the other hand, the quantification of DTG and other drugs in LNMCs needs cell isolation steps with aqueous buffers (e.g., use of cell strainers with cell washings) [31], which are potentially associated with drug loss from the cells, possibly leading to underestimation of DTG concentrations.

Interestingly, the observed LNs-to-plasma concentrations ratios for DTG were comparable (0.59 vs. 0.44) with other studies that considered lymphoid tissue homogenates, such as that by Weber et al. on gut-associated lymphoid tissue (GALT) [47]. Conversely, concerning TFV–DP and FTC–TP, there is a less significant impact of the extracellular matrix on the intracellular quantification, as these

Table 3
Descriptive statistics stratified by randomisation arm, in patients with early (I–II) Fiebig stages. *P*-values refer to Kruskal-Wallis or Chi-square tests for continuous and categorical variables, respectively.

Factors	Level/Unit	Fiebig I–II			*P*-value
		TAF/FTC + DRV N=6	TAF/FTC + DTG N=6	TAF/FTC + DRV + DTG N=5	
Sex (%)	F	1 (16.7)	0 (0.0)	0 (0.0)	0.378
	M	5 (83.3)	6 (100.0)	5 (100.0)	
Age (median [IQR])	years	32.1 [28.8–40.4]	39.3 [33.7–48.2]	44.8 [36.7–47.3]	0.714
HBsAg (%)	no	6 (100.0)	6 (100.0)	5 (100.0)	NA
HCV (%)	no	6 (100.0)	6 (100.0)	5 (100.0)	NA
median CD4 BL [IQR]	Cells/mm^3	779 [633–794]	570 [500–658]	567 [472–677]	0.37
median CD4 w12 [IQR]	Cells/mm^3	745 [606–885]	546 [496–599]	642 [515–689]	0.134
median CD4 w24 [IQR]	Cells/mm^3	721 [616–842]	630 [570–640]	659 [523–707]	0.61
median CD4 w24 [IQR]	Cells/mm^3	957 [813–1065]	730 [712–809]	665 [538–714]	0.088
median CD4 w48 [IQR]	Cells/mm^3	880 [768–1016]	685 [609–712]	596 [529–643]	0.056
median HIV RNA BL [IQR]	Log_{10} cps/mL	6.89 [6.28–7.00]	6.61 [6.50–6.91]	7.00 [6.11–7.00]	0.916
median HIV RNA w2 [IQR]	Log_{10} cps/mL	3.89 [3.39–5.15]	3.82 [3.22–4.41]	3.24 [2.65–3.55]	0.405
median HIV RNA w4 [IQR]	Log_{10} cps/mL	3.37 [3.06–4.11]	2.85 [2.35–3.51]	2.36 [2.35–2.73]	0.194
median HIV RNA w8 [IQR]	Log_{10} cps/mL	3.03 [1.80–4.03]	2.52 [1.81–2.66]	2.04 [1.49–2.06]	0.299
median HIV RNA w12 [IQR]	Log_{10} cps/mL	2.26 [1.44–3.22]	2.19 [1.80–2.31]	1.53 [1.48–1.65]	0.184
median HIV RNA w24 [IQR]	Log_{10} cps/mL	1.74 [1.38–2.61]	2.10 [1.72–2.15]	1.48 [1.41–1.51]	0.52
median HIV RNA w36 [IQR]	Log_{10} cps/mL	1.39 [1.30–2.25]	1.79 [1.60–2.09]	1.30 [1.30–1.48]	0.199
median HIV RNA w48 [IQR]	Log_{10} cps/mL	1.48 [1.30–1.60]	1.61 [1.60–1.67]	1.48 [1.30–1.51]	0.4
median HIV DNA BL [IQR]	Log_{10} cps/10^6 PBMCs	4.18 [3.91–4.82]	4.42 [4.17–4.73]	4.49 [4.45–4.77]	0.777
median HIV DNA w12 [IQR]	Log_{10} cps/10^6 PBMCs	3.68 [3.50–4.10]	3.96 [3.41–4.18]	4.24 [3.85–4.34]	0.612
median HIV DNA w48 [IQR]	Log_{10} cps/10^6 PBMCs	3.49 [0.83–3.74]	3.82 [3.24–4.18]	3.57 [1.78–3.84]	0.486

Table 4
Descriptive statistics stratified by randomisation arm–in patients with later (III–VI) Fiebig stages. *P*-values refer to Kruskal-Wallis or Chi-square tests for continuous and categorical variables–respectively.

Factors	Level/Unit	Fiebig stages III–VI			*P*- value
		TAF/FTC + DRV N=20	TAF/FTC + DTG N=21	TAF/FTC + DRV + DTG N=13	
Sex (%)	F	2 (10.0)	0 (0.0)	0 (0.0)	0.171
	M	18 (90.0)	21 (100.0)	13 (100.0)	
Median age, years [IQR]		34.64 [29.62–44.13]	31.56 [27.75–37.76]	32.48 [27.25–46.28]	0.769
HBsAg (%)	no	19 (100.0)	20 (100.0)	11 (100.0)	NA
HCV (%)	no	17 (94.4)	18 (94.7)	12 (100.0)	0.712
	yes	1 (5.6)	1 (5.3)	0 (0.0)	
median CD4 BL [IQR]	Cells/mm^3	524 [444–722]	706 [517–915]	687 [482–781]	0.296
median CD4 w12 [IQR]	Cells/mm^3	613 [449–815]	720 [472–920]	641 [590–885]	0.784
median CD4 w24 [IQR]	Cells/mm^3	580 [508–668]	706.00 [531–805]	742 [545–940]	0.21
median CD4 w24 [IQR]	Cells/mm^3	676 [557–877]	836 [618–1003]	842 [611–968]	0.357
median CD4 w48 [IQR]	Cells/mm^3	695 [567–887]	683 [561–980]	715 [519–1004]	0.988
median HIV RNA BL [IQR]	Log_{10} cps/mL	4.86 [4.17–5.75]	5.28 [4.26–5.74]	5.95 [4.88–6.29]	0.196
median HIV RNA w2 [IQR]	Log_{10} cps/mL	3.45 [2.68–3.92]	2.16 [1.82–2.64]	2.79 [2.46–3.07]	0.002
median HIV RNA w4 [IQR]	Log_{10} cps/mL	3.22 [2.54–3.57]	1.65 [1.39–2.19]	2.13 [1.98–2.18]	<0.001
median HIV RNA w8 [IQR]	Log_{10} cps/mL	2.74 [2.09–3.05]	1.49 [1.30–1.60]	1.60 [1.55–1.81]	<0.001
median HIV RNA w12 [IQR]	Log_{10} cps/mL	2.20 [1.61–2.47]	1.30 [1.30–1.57]	1.60 [1.57–2.15]	0.001
median HIV RNA w24 [IQR]	Log_{10} cps/mL	1.60 [1.30–1.89]	1.30 [1.30–1.55]	1.56 [1.30–1.62]	0.132
median HIV RNA w36 [IQR]	Log_{10} cps/mL	1.30 [1.30–1.39]	1.30 [1.30–1.40]	1.57 [1.30–1.63]	0.255
median HIV RNA w48 [IQR]	Log_{10} cps/mL	1.30 [1.30–1.35]	1.30 [1.30–1.39]	1.30 [1.30–1.61]	0.761
median HIV DNA BL [IQR]	Log_{10} cps/10^6 PBMCs	4.39 [4.01–4.66]	4.57 [4.14–4.88]	4.40 [4.08–4.93]	0.702
median HIV DNA w12 [IQR]	Log_{10} cps/10^6 PBMCs	4.12 [3.83–4.31]	4.34 [3.96–4.63]	4.29 [3.80–4.56]	0.228
median HIV DNA w48 [IQR]	Log_{10} cps/10^6 PBMCs	3.90 [3.62–4.53]	3.95 [3.52–4.44]	4.16 [3.78–4.38]	0.893

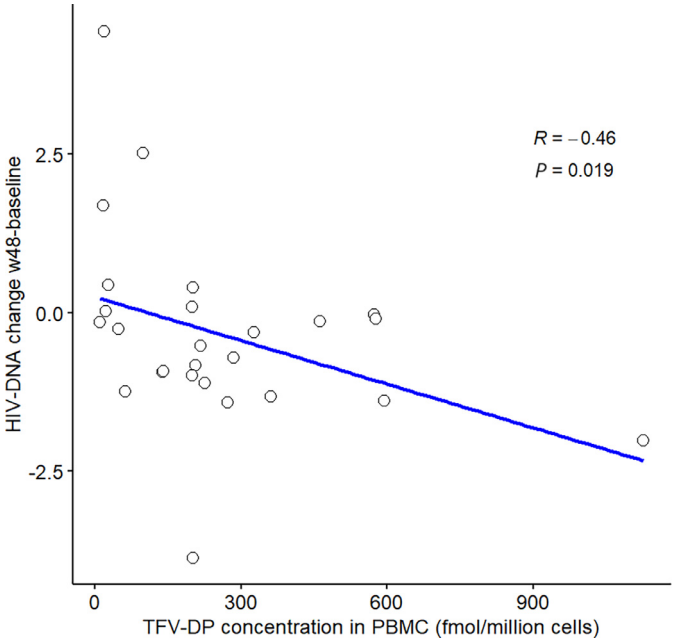

Figure 3. Correlation between the HIV DNA change during the study period and the intra-PBMC TFV–DP concentration in the group of patients with higher Fiebig stages (Fiebig III–VI).

metabolites are only produced and tend to remain within the cells, due to their highly hydrophilic nature. Interestingly, only TFV–DP concentrations in PBMCs showed a significant association with HIV DNA decay after 48 weeks of treatment, in accordance with previous reports [31,36,48]. TAF is a prodrug specifically designed to show high PBMC-to-plasma accumulation ratios. Moreover, TFV–DP, the active intracellular moiety, has a well-known long half-life (range 30–72 h), which makes it a marker of the overall exposure to treatment [40,49,50]. Therefore, combining these characteristics, the correlation between HIV DNA decay and TFV–DP accumulation within PBMCs may be explained by a higher cumulative exposure to TAF, including higher overall bioavailability (absorption and first-pass metabolism) and/or higher adherence during the study period [49]. Moreover, the impact of TFV–DP concentrations in PBMCs was significant only in the group of participants with more advanced Fiebig stages (III–VI). This indicates that a higher HIV DNA decay can be achieved with extremely early treatment, irrespective of drug concentrations, whereas higher PK exposure may be required to achieve a similar goal in less recent infections.

There was a gradual trend for DTG concentrations in plasma and PBMCs to increase over time throughout the protocol. Considering that all the measurements were made at steady state, this trend may be explained by a gradual change in the inflammatory status in these patients, in accordance with previous reports [35,51].

Nevertheless, the present study has some limitations. The PK evaluation was performed in only a small subset of patients (n=9) in LNs, due to the invasive sampling. The quantification in LNs was performed in tissue homogenates, including different cell types and interstitial fluid, and was therefore not comparable with previously described drug concentrations in LNMCs. Total HIV DNA was quantified, which is expected to be the most reliable from a quantitative point of view [7,10,52], but we cannot infer about its replication competency. Finally, the overall relatively low number of patients and the inhomogeneous treatments do not allow enough stratification to draw definitive conclusions.

In conclusion, the present study indicates variable penetration of ARVs in PBMCs and LNs, confirming higher penetration and impact on HIV DNA reservoir for TFV–DP, particularly compared with DTG and DRV. It is worth noting that this correlation emerges later during the follow-up (at 48 weeks) and is particularly marked in patients with less recent PHI (Fiebig III–VI), indicating a cumulative and slow effect of TFV–DP on HIV DNA during the first year of treatment. Moreover, the observed correlation between HIV DNA change and TFV–DP might be explained by a mutual correlation with a third genetic or immunological factor that was not observed in the current study. This latter point deserves further investigation. On the other hand, extremely early treatment, during Fiebig stages I–II, overcomes the impact of treatment regimens and ARV

PK in PBMCs on HIV DNA decay, highlighting the timing of treatment initiation and the treatment itself (regimen and exposure) as primary and secondary factors, respectively, to affect HIV reservoir.

Acknowledgements and Funding

The authors would like to thank the study participants.

Declarations

Funding: The authors would like to thank the Ministry of Health for the financial support (Grant NET-2013-02355333).

Competing Interests: Amedeo De Nicolò, Alice Palermiti, Stefania Dispinseri, Elena Bruzzesi, Arianna Gabrieli, Mattia Trunfio, Elisa De Vivo, Antonio D'Avolio and Davide Paolo Bernasconi have no conflict of interest to declare. Silvia Nozza, Stefano Rusconi, Giulia Marchetti, Andrea Calcagno, Antonio Muscatello, Alessandra Bandera, received fees for Advisory Boards and consultations from ViiV Healthcare.

Ethical Approval: The study was approved by the Ethical Committee, Ospedale San Raffaele, Milan, Italy. All participants signed informed consent.

Sequence Information: No.

Randomized Controlled Trial: This study is registered under the number NCT04225325 on ClinicalTrials.gov.

Data Availability Statement: The data that support the findings of this study are available on request from the corresponding author. The data are not publicly available due to privacy or ethical restrictions.

Supplementary materials

Supplementary material associated with this article can be found, in the online version, at doi:10.1016/j.ijantimicag.2024.107200.

References

[1] Bachmann N, von Siebenthal C, Vongrad V, Turk T, Neumann K, Beerenwinkel N, et al. Determinants of HIV-1 reservoir size and long-term dynamics during suppressive ART. Nat Commun 2019;10:3193 [pii]. doi:10.1038/s41467-019-10884-9.
[2] Churchill MJ, Deeks SG, Margolis DM, Siliciano RF, Swanstrom R. HIV reservoirs: what, where and how to target them. Nat Rev Microbiol 2015;14:55–60 nrmicro.2015.5 [pii]. doi:10.1038/nrmicro.2015.5.
[3] Finzi D, Blankson J, Siliciano JD, Margolick JB, Chadwick K, Pierson T, et al. Latent infection of CD4+ T cells provides a mechanism for lifelong persistence of HIV-1, even in patients on effective combination therapy. Nat Med 1999;5:512–17. doi:10.1038/8394.
[4] Rose R, Nolan DJ, Maidji E, Stoddart CA, Singer EJ, Lamers SL, et al. Eradication of HIV from tissue reservoirs: challenges for the cure. AIDS Res Hum Retroviruses 2017;34:3–8. doi:10.1089/aid.2017.0072.
[5] Chomont N, El-Far M, Ancuta P, Trautmann L, Procopio FA, Yassine-Diab B, et al. HIV reservoir size and persistence are driven by T cell survival and homeostatic proliferation. Nat Med 2009;15:893–900 nm.1972.
[6] Mzingwane ML, Tiemessen CT. Mechanisms of HIV persistence in HIV reservoirs. Rev Med Virol 2017;27. doi:10.1002/rmv.1924.
[7] Alteri C, Scutari R, Stingone C, Maffongelli G, Brugneti M, Falasca F, et al. Quantification of HIV-DNA and residual viremia in patients starting ART by droplet digital PCR: their dynamic decay and correlations with immunological parameters and virological success. J Clin Virol 2019;117:61–7 S1386-6532(19)30142-8. doi:10.1016/j.jcv.2019.06.004.
[8] Thompson CG, Gay CL, Kashuba ADM. HIV persistence in gut-associated lymphoid tissues: pharmacological challenges and opportunities. AIDS Res Hum Retroviruses 2017;33:513–23. doi:10.1089/aid.2016.0253.
[9] Lorenzo-Redondo R, Fryer HR, Bedford T, Kim EY, Archer J, Pond SLK, et al. Persistent HIV-1 replication maintains the tissue reservoir during therapy. Nature 2016;530:51–6. doi:10.1038/nature16933.
[10] Besson GJ, Lalama CM, Bosch RJ, Gandhi RT, Bedison MA, Aga E, et al. HIV-1 DNA decay dynamics in blood during more than a decade of suppressive antiretroviral therapy. Clin Infect Dis 2014;59:1312–21. doi:10.1093/cid/ciu585.
[11] Lau CY, Adan MA, Maldarelli F. Why the HIV reservoir never runs dry: clonal expansion and the characteristics of HIV-infected cells challenge strategies to cure and control HIV infection. Viruses 2021;13. doi:10.3390/v13122512.
[12] Fidler S, Stohr W, Pace M, Dorrell L, Lever A, Pett S, et al. Antiretroviral therapy alone versus antiretroviral therapy with a kick and kill approach, on measures of the HIV reservoir in participants with recent HIV infection (the RIVER trial): a phase 2, randomised trial. Lancet 2020;395:888–98. doi:10.1016/S0140-6736(19)32990-3.
[13] Lewin SR, Rasmussen TA. Kick and kill for HIV latency. Lancet 2020;395:844–6. doi:10.1016/S0140-6736(20)30264-6.
[14] Li C, Mori L, Valente ST. The block-and-lock strategy for human immunodeficiency virus cure: lessons learned from didehydro-cortistatin A. J Infect Dis 2021;223:46–53. doi:10.1093/infdis/jiaa681.
[15] Mediouni S, Lyu S, Schader SM, Valente ST. Forging a Functional Cure for HIV: Transcription Regulators and Inhibitors. Viruses 2022;14. doi:10.3390/v14091980.
[16] Vansant G, Bruggemans A, Janssens J, Debyser Z. Block-And-lock strategies to cure HIV infection. Viruses 2020;12. doi:10.3390/v12010084.
[17] Dash PK, Chen C, Kaminski R, Su H, Mancuso P, Sillman B, et al. CRISPR editing of CCR5 and HIV-1 facilitates viral elimination in antiretroviral drug-suppressed virus-infected humanized mice. Proc Natl Acad Sci U S A 2023;120:e2217887120. doi:10.1073/pnas.2217887120.
[18] Freen-van Heeren JJ. Closing the door with CRISPR: genome editing of CCR5 and CXCR4 as a potential curative solution for HIV. BioTech (Basel) 2022;11. doi:10.3390/biotech11030025.
[19] Fletcher CV, Podany AT, Thorkelson A, Winchester LC, Mykris T, Anderson J, et al. The lymphoid tissue pharmacokinetics of tenofovir disoproxil fumarate and tenofovir alafenamide in HIV-infected persons. Clin Pharmacol Ther 2020;108:971–5. doi:10.1002/cpt.1883.
[20] Tincati C, Biasin M, Bandera A, Violin M, Marchetti G, Piacentini L, et al. Early initiation of highly active antiretroviral therapy fails to reverse immunovirological abnormalities in gut-associated lymphoid tissue induced by acute HIV infection. Antivir Ther 2009;14:321–30.
[21] Allers K, Hutter G, Hofmann J, Loddenkemper C, Rieger K, Thiel E, et al. Evidence for the cure of HIV infection by CCR5Delta32/Delta32 stem cell transplantation. Blood 2010;117:2791–9. doi:10.1182/blood-2010-09-309591.
[22] Gupta RK, Peppa D, Hill AL, Galvez C, Salgado M, Pace M, et al. Evidence for HIV-1 cure after CCR5Delta32/Delta32 allogeneic haemopoietic stem-cell transplantation 30 months post analytical treatment interruption: a case report. Lancet HIV 2020;7:e340–7. doi:10.1016/S2352-3018(20)30069-2.
[23] Hsu J, Van Besien K, Glesby MJ, Pahwa S, Coletti A, Warshaw MG, et al. HIV-1 remission and possible cure in a woman after haplo-cord blood transplant. Cell 2023;186:1115–26 e8. doi:10.1016/j.cell.2023.02.030.
[24] Jensen BO, Knops E, Cords L, Lubke N, Salgado M, Busman-Sahay K, et al. In-depth virological and immunological characterization of HIV-1 cure after CCR5Delta32/Delta32 allogeneic hematopoietic stem cell transplantation. Nat Med 2023;29:583–7. doi:10.1038/s41591-023-02213-x.
[25] Ananworanich J, Chomont N, Eller LA, Kroon E, Tovanabutra S, Bose M, et al. HIV DNA set point is rapidly established in acute HIV infection and dramatically reduced by early ART. EBioMedicine 2016;11:68–72. doi:10.1016/j.ebiom.2016.07.024.
[26] Schmid A, Gianella S, von Wyl V, Metzner KJ, Scherrer AU, Niederost B, et al. Profound depletion of HIV-1 transcription in patients initiating antiretroviral therapy during acute infection. PLoS One 2010;5:e13310. doi:10.1371/journal.pone.0013310.
[27] Cockerham LR, Hatano H, Deeks SG. Post-treatment controllers: role in HIV "cure" research. Curr HIV/AIDS Rep 2016;13:1–9 [pii] 10.1007/s11904-016-0296-x. doi:10.1007/s11904-016-0296-x.
[28] Saez-Cirion A, Bacchus C, Hocqueloux L, Avettand-Fenoel V, Girault I, Lecuroux C, et al. Post-treatment HIV-1 controllers with a long-term virological remission after the interruption of early initiated antiretroviral therapy ANRS VISCONTI Study. PLoS Pathog 2013;9:e1003211. doi:10.1371/journal.ppat.1003211.
[29] Cheret A, Nembot G, Melard A, Lascoux C, Slama L, Miailhes P, et al. Intensive five-drug antiretroviral therapy regimen versus standard triple-drug therapy during primary HIV-1 infection (OPTIPRIM-ANRS 147): a randomised, open-label, phase 3 trial. Lancet Infect Dis 2015;15:387–96. doi:10.1016/S1473-3099(15)70021-6.
[30] Fletcher CV, Kroon E, Schacker T, Pinyakorn S, Chomont N, Chottanapund S, et al. Persistent HIV transcription and variable antiretroviral drug penetration in lymph nodes during plasma viral suppression. AIDS 2022;36:985–90. doi:10.1097/QAD.0000000000003201.
[31] Fletcher CV, Staskus K, Wietgrefe SW, Rothenberger M, Reilly C, Chipman JG, et al. Persistent HIV-1 replication is associated with lower antiretroviral drug concentrations in lymphatic tissues. Proc Natl Acad Sci U S A 2014;111:2307–12. doi:10.1073/pnas.1318249111.
[32] Riggs PK, Chaillon A, Jiang G, Letendre SL, Tang Y, Taylor J, et al. Lessons for understanding central nervous system HIV reservoirs from the Last Gift Program. Curr HIV/AIDS Rep 2022;19:566–79. doi:10.1007/s11904-022-00628-8.
[33] Chun TW, Carruth L, Finzi D, Shen X, DiGiuseppe JA, Taylor H, et al. Quantification of latent tissue reservoirs and total body viral load in HIV-1 infection. Nature 1997;387:183–8. doi:10.1038/387183a0.

[34] Sanchez JL, Hunt PW, Reilly CS, Hatano H, Beilman GJ, Khoruts A, et al. Lymphoid fibrosis occurs in long-term nonprogressors and persists with antiretroviral therapy but may be reversible with curative interventions. J Infect Dis 2014;211:1068–75. doi:10.1093/infdis/jiu586.
[35] Ferrara M, Cusato J, Salvador E, Trentalange A, Alcantarini C, Trunfio M, et al. Inflammation and intracellular exposure of dolutegravir, darunavir, tenofovir and emtricitabine in people living with HIV. Br J Clin Pharmacol 2022;89:1020–6. doi:10.1111/bcp.15538.
[36] Burgunder E, Fallon JK, White N, Schauer AP, Sykes C, Remling-Mulder L, et al. Antiretroviral drug concentrations in lymph nodes: a cross-species comparison of the effect of drug transporter expression, viral infection, and sex in humanized mice, nonhuman primates, and humans. J Pharmacol Exp Ther 2019;370:360–8. doi:10.1124/jpet.119.259150.
[37] Rosen EP, Deleage C, White N, Sykes C, Brands C, Adamson L, et al. Antiretroviral drug exposure in lymph nodes is heterogeneous and drug dependent. J Int AIDS Soc 2022;25:e25895. doi:10.1002/jia2.25895.
[38] Dyavar SR, Gautam N, Podany AT, Winchester LC, Weinhold JA, Mykris TM, et al. Assessing the lymphoid tissue bioavailability of antiretrovirals in human primary lymphoid endothelial cells and in mice. J Antimicrob Chemother 2019;74:2974–8. doi:10.1093/jac/dkz273.
[39] Bruzzesi E, Gabrieli A, Bernasconi D, Marchetti G, Calcagno A, Ripamonti D, et al. HIV-DNA decrease during treatment in primary HIV-1 infection with three different drug regimens: Italian Network of Acute HIV Infection (INACTION) clinical trial. J Med Virol 2023;95:e29114. doi:10.1002/jmv.29114.
[40] Thurman AR, Schwartz JL, Cottrell ML, Brache V, Chen BA, Cochon L, et al. Safety and pharmacokinetics of a tenofovir alafenamide fumarate-emtricitabine based oral antiretroviral regimen for prevention of HIV acquisition in women: a randomized controlled trial. EClinicalMedicine 2021;36:100893. doi:10.1016/j.eclinm.2021.100893.
[41] De Nicolò A, Calcagno A, Motta I, De Vivo E, D'Avolio A, Di Perri G, et al. The effect of rifampicin on darunavir, ritonavir, and dolutegravir exposure within peripheral blood mononuclear cells: a dose escalation study. Antimicrob Agents Chemother 2022;66:e0013622. doi:10.1128/aac.00136-22.
[42] De Nicolò A, Ianniello A, Ferrara M, Avataneo V, Cusato J, Antonucci M, et al. Validation of a UHPLC-MS/MS method to quantify twelve antiretroviral drugs within peripheral blood mononuclear cells from people living with HIV. Pharmaceuticals (Basel) 2020;14. doi:10.3390/ph14010012.
[43] De Nicolò A, Manca A, Ianniello A, Palermiti A, Calcagno A, Ferrara M, et al. Development and validation of an up-to-date highly sensitive UHPLC-MS/MS method for the simultaneous quantification of current anti-HIV nucleoside analogues in human plasma. Pharmaceuticals (Basel) 2021;14. doi:10.3390/ph14050460.
[44] Simiele M, Ariaudo A, De Nicolo A, Favata F, Ferrante M, Carcieri C, et al. UPLC-MS/MS method for the simultaneous quantification of three new antiretroviral drugs, dolutegravir, elvitegravir and rilpivirine, and other thirteen antiretroviral agents plus cobicistat and ritonavir boosters in human plasma. J Pharm Biomed Anal 2017;138:223–30. doi:10.1016/j.jpba.2017.02.002.
[45] Ziyade S, Pinarbasili NB, Ziyade N, Akdemir OC, Sahin F, Soysal O, et al. Determination of standard number, size and weight of mediastinal lymph nodes in postmortem examinations: reflection on lung cancer surgery. J Cardiothorac Surg 2013;8:94. doi:10.1186/1749-8090-8-94.
[46] Podany AT, Bares SH, Havens J, Dyavar SR, O'Neill J, Lee S, et al. Plasma and intracellular pharmacokinetics of tenofovir in patients switched from tenofovir disoproxil fumarate to tenofovir alafenamide. AIDS 2018;32:761–5. doi:10.1097/QAD.0000000000001744.
[47] Weber MD, Andrews E, Prince HA, Sykes C, Rosen EP, Bay C, et al. Virological and immunological responses to raltegravir and dolutegravir in the gut-associated lymphoid tissue of HIV-infected men and women. Antivir Ther 2018;23:495–504. doi:10.3851/IMP3236.
[48] Ruane PJ, DeJesus E, Berger D, Markowitz M, Bredeek UF, Callebaut C, et al. Antiviral activity, safety, and pharmacokinetics/pharmacodynamics of tenofovir alafenamide as 10-day monotherapy in HIV-1-positive adults. J Acquir Immune Defic Syndr 2013;63:449–55. doi:10.1097/QAI.0b013e3182965d45.
[49] Yager JL, Brooks KM, Castillo-Mancilla JR, Nemkov C, Morrow M, Peterson S, et al. Tenofovir-diphosphate in peripheral blood mononuclear cells during low, medium and high adherence to emtricitabine/tenofovir alafenamide vs. emtricitabine/tenofovir disoproxil fumarate. AIDS 2021;35:2481–7. doi:10.1097/QAD.0000000000003062.
[50] Cottrell ML, Garrett KL, Prince HMA, Sykes C, Schauer A, Emerson CW, et al. Single-dose pharmacokinetics of tenofovir alafenamide and its active metabolite in the mucosal tissues. J Antimicrob Chemother 2017;72:1731–40. doi:10.1093/jac/dkx064.
[51] Minuesa G, Arimany-Nardi C, Erkizia I, Cedeno S, Molto J, Clotet B, et al. P-Glycoprotein (ABCB1) activity decreases raltegravir disposition in primary CD4+P-gphigh cells and correlates with HIV-1 viral load. J Antimicrob Chemother 2016;71:2782–92. doi:10.1093/jac/dkw215.
[52] Kiselinova M, De Spiegelaere W, Buzon MJ, Malatinkova E, Lichterfeld M, Vandekerckhove L. Integrated and total HIV-1 DNA predict ex vivo viral outgrowth. PLoS Pathog 2016;12:e1005472. doi:10.1371/journal.ppat.1005472.